Energy-Conserving Theory of the Blowout Regime of Plasma Wakefield

A. Golovanov,[1,2,*] I. Yu. Kostyukov,[2,3] A. Pukhov,[4] and V. Malka[1]
[1]*Weizmann Institute of Science, 7610001 Rehovot, Israel*
[2]*Institute of Applied Physics RAS, 603950 Nizhny Novgorod, Russia*
[3]*Lobachevsky State University of Nizhny Novgorod, 603022 Nizhny Novgorod, Russia*
[4]*Institut für Theoretische Physik I, Heinrich-Heine-Universität Düsseldorf, 40225 Düsseldorf, Germany*

(Received 28 August 2022; accepted 6 February 2023; published 7 March 2023)

We present a self-consistent theory of strongly nonlinear plasma wakefield (bubble or blowout regime of the wakefield) based on the energy conservation approach. Such wakefields are excited in plasmas by intense laser or particle beam drivers and are characterized by the expulsion of plasma electrons from the propagation axis of the driver. As a result, a spherical cavity devoid of electrons (called a "bubble") and surrounded by a thin sheath made of expelled electrons is formed behind the driver. In contrast to the previous theoretical model [W. Lu *et al.*, Phys. Rev. Lett. **96**, 165002 (2006)], the presented theory satisfies the energy conservation law, does not require any external fitting parameters, and describes the bubble structure and the electromagnetic field it contains with much higher accuracy in a wide range of parameters. The obtained results are verified by 3D particle-in-cell simulations.

DOI: 10.1103/PhysRevLett.130.105001

Plasma accelerators are promising for achieving high acceleration gradients and pave the way to creating compact particle accelerators [1–3] by using the strong longitudinal electric field (wakefield) of plasma wake waves to accelerate particles to high energies. With the wake phase velocity being close to the speed of light, the accelerated relativistic particles can stay in the accelerating phase of the wake and efficiently gain energy. The two methods of plasma acceleration are laser-wakefield acceleration (LWFA) in which a short intense laser pulse is used to drive a wake wave in an underdense plasma [4] and plasma-wakefield acceleration based on particle drivers [5]. For femtosecond laser pulses with high enough intensity, which are currently available at many laser facilities, the laser-plasma interaction happens in the strongly nonlinear [6] regime in which the laser pulse completely expels plasma electrons from its propagation axis, leading to the formation of a spherical cavity (called a "bubble") devoid of plasma electrons [7]. This promising regime for electron acceleration allows high accelerating gradients, facilitates self-injection, and leads to the generation of quasimonoenergetic bunches without an external electron source [8–10]. The current record energy achieved in LWFA in this regime is 8 GeV at a distance of 20 cm [11]. The same effect of a bubble formation is observed in plasma-wakefield acceleration with dense bunches (see Fig. 1) [12].

Because of the highly nonlinear nature of the interaction, theoretical description of the bubble or blowout regime of plasma wakefield remains challenging. Several early phenomenological models were able to qualitatively describe the properties of the bubble regime [13,14]. A major breakthrough was achieved in the model proposed by Lu *et al.* [15,16] where the equation describing the boundary of the bubble was derived. Later this model has seen several important developments, including estimations of the beam loading influence [17], alternative shapes for the electron

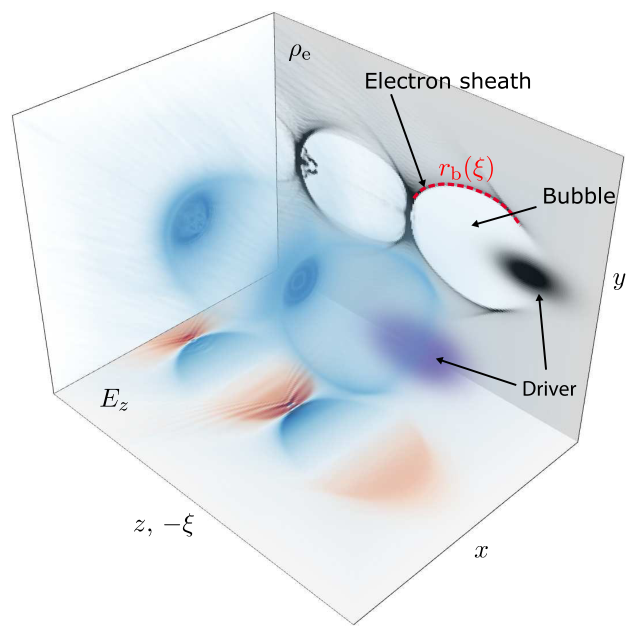

FIG. 1. Schematic depiction of a bubble excited by an electron driver (purple) in a plasma. Planar projections show the distributions of the electron density ρ_e in plasma and the longitudinal electric field E_z (blue corresponds to regions of acceleration $E_z < 0$, red to deceleration $E_z > 0$) in the central slices.

sheath [18,19], generalization to plasmas with transverse inhomogeneous profiles [20,21], a multisheath model that more accurately fits numerical simulations [22], and a method for calculating the bubble excitation by an electron driver [23]. However, these models either require fitting parameters (such as the thickness of the electron sheath at the boundary of the bubble) which can be only estimated from numerical simulations or are applicable only in some limiting cases.

In this Letter, we propose a different approach based on the energy conservation law. We derive a new equation for the boundary of the bubble and demonstrate that it more accurately describes the bubble regime over a wide range of parameters. This new approach does not rely on additional fitting parameters, and the better suitability is due to its energy-conserving properties. For the sake of coherence, we also extend the new approach to the bubble excitation by an electron bunch.

The plasma wakefield consists of two components carrying energy: the electromagnetic (EM) field and electrons. We consider noncollisional plasmas and immobile ions, thus neglecting their contribution to the total energy. The electromagnetic field energy conservation law corresponds to Poynting's theorem,

$$\frac{\partial W_{\mathrm{EM}}}{\partial t} + \boldsymbol{\nabla} \cdot \boldsymbol{S}_{\mathrm{EM}} = -\boldsymbol{j} \cdot \boldsymbol{E}, \tag{1}$$

where $W_{\mathrm{EM}} = \frac{1}{2}(\boldsymbol{E}^2 + \boldsymbol{B}^2)$ is the EM energy density, $\boldsymbol{S}_{\mathrm{EM}} = \boldsymbol{E} \times \boldsymbol{B}$ is the Poynting vector, and $\boldsymbol{j}$ is the spatial distribution of the current charge density. Assuming there are no collisions, a similar equation can be written for plasma electrons,

$$\frac{\partial W_e}{\partial t} + \boldsymbol{\nabla} \cdot \boldsymbol{S}_e = \boldsymbol{j}_e \cdot \boldsymbol{E} + \frac{1}{2}\frac{\partial \langle \boldsymbol{a}^2 \rangle}{\partial t} n_e \overline{\gamma^{-1}}, \tag{2}$$

where $W_e = n_e(\bar{\gamma} - 1)$ is the electron energy density, and $\boldsymbol{S}_e = n_e(\bar{\boldsymbol{p}} - \bar{\boldsymbol{v}})$ is the energy current. Here, the horizontal bars correspond to averaging over the electron distribution function in the momentum space. We use the ponderomotive description for the laser driver in which its force depends on the time-averaged square $\langle \boldsymbol{a}^2 \rangle$ of dimensionless laser amplitude $\boldsymbol{a} = e\boldsymbol{E}/(mc\omega_L)$, where ω_L is the laser frequency [24]. Fields $\boldsymbol{E}$ and $\boldsymbol{B}$ and therefore the energy density W_{EM} thus correspond only to plasma fields.

All equations in this Letter are written in plasma units, in which time is normalized to ω_p^{-1}, coordinates to c/ω_p, electric and magnetic fields to $mc\omega_p/e$, velocities to c, momenta to mc, electron energies to mc^2, electron density to n_p, where m is the electron mass, $e > 0$ is the elementary charge, c is the speed of light, n_p is the unperturbed electron density, and $\omega_p = (4\pi e^2 n_p/m)^{1/2}$ is the electron plasma frequency. The dimensional values here are given in Gaussian units.

As the wakefield driver moves along the z direction with the speed close to the speed of light and evolves slowly, we can use the quasistatic approximation [25] and replace the time t and the longitudinal coordinate z with the copropagating coordinate $\xi = t - z$. In this case, the energy conservation law for the total energy $W = W_{\mathrm{EM}} + W_e$ and total energy flow $\boldsymbol{S} = \boldsymbol{S}_{\mathrm{EM}} + \boldsymbol{S}_e$ can be written as

$$\frac{\partial \tilde{W}}{\partial \xi} + \boldsymbol{\nabla}_\perp \cdot \boldsymbol{S}_\perp = -\rho_B E_z + \frac{1}{2}\frac{\partial \langle \boldsymbol{a}^2 \rangle}{\partial \xi} n_e \overline{\gamma^{-1}}, \tag{3}$$

where $\tilde{W} = W - S_z$, which we refer to as the quasienergy density of plasma wake. The sources on the right-hand side correspond to relativistic bunches (both drivers and witnesses) with the current $\boldsymbol{j}_B = \boldsymbol{j} - \boldsymbol{j}_e \approx \rho_B \boldsymbol{z}_0$ and the laser driver. This equation is similar to the energy conservation law in the transverse 2D space with ξ acting as a time variable.

Plasma wakefields are usually described with the wakefield potential $\psi = \varphi - A_z$, where φ is the electrostatic potential, and A_z is the z component of the vector potential $\boldsymbol{A}$. In this case, the wakefield is fully represented with the magnetic field $\boldsymbol{B}$ and the wakefield potential ψ, and the electric field can be written as $\boldsymbol{E} = -\boldsymbol{\nabla}\psi - \boldsymbol{z}_0 \times \boldsymbol{B}$, and the quasienergy densities of the EM field and electrons are $\tilde{W}_{\mathrm{EM}} = \frac{1}{2}[(\boldsymbol{\nabla}\psi)^2 + B_z^2]$ and $\tilde{W}_e = n_e\overline{(\gamma - 1)(1 - v_z)}$, respectively. Both $\tilde{W}_{\mathrm{EM}}$ and $\tilde{W}_e$ are positively defined values, which supports their meaning as quasienergy density.

If we integrate Eq. (3) over the transverse coordinate, we get

$$\frac{d\Psi}{d\xi} = -\int \rho_B E_z d^2\boldsymbol{r}_\perp + \frac{1}{2}\int \frac{\partial \langle \boldsymbol{a}^2 \rangle}{\partial \xi} n_e \overline{\gamma^{-1}} d^2\boldsymbol{r}_\perp, \tag{4}$$

where $\Psi(\xi) = \int \tilde{W}(\xi, \boldsymbol{r}_\perp) d^2\boldsymbol{r}_\perp$ is total quasienergy in the transverse 2D slice ($\xi = \mathrm{const}$) or, alternatively, the total energy flux along the moving window [14]. This equation describes the exchange of the quasienergy stored in the wakefield with laser drivers and external particle bunches. In the regions along ξ where the right-hand side is equal to 0 (for example, behind the driver and in the absence of accelerated witness bunches), $\Psi = \mathrm{const}$, so quasienergy is conserved in a wakefield. This energy conservation is general and must be satisfied in all cases, including the case of strongly nonlinear interaction, so we can expect that the properties of the bubble should be related to energy conservation.

We now consider the strongly nonlinear regime of interaction in uniform plasma. We assume axial symmetry, so all values depend on $r = |\boldsymbol{r}_\perp|$, and only E_z, E_r, and B_ϕ components of the EM field remain nonzero. For simplicity, we also ignore the influence of the laser pulse, assuming that we consider either an electron driver or LWFA in the region behind the laser driver, where its influence is no longer present.

Before moving on to applying the energy conservation law to the bubble regime, we briefly describe the existing theory of this regime by W. Lu *et al.* [15,16], as the comparison to it will be important. In this theory, the space is separated into three different areas: the inner part of the bubble with a radius $r_b(\xi)$ that depends on the longitudinal coordinate, the electron sheath at the boundary of the bubble, and the unperturbed plasma far outside the bubble (see Fig. 1). The boundary of the bubble $r_b(\xi)$ is then treated as an electron trajectory, which leads to a second-order ordinary differential equation,

$$A(r_b)\frac{d^2 r_b}{d\xi^2} + B(r_b)\left(\frac{dr_b}{d\xi}\right)^2 + C(r_b) = \lambda(\xi, r_b) \quad (5)$$

and the electric field is $E_z = \alpha(r_b)dr_b/d\xi$, where

$$A = \frac{r_b^3}{4} + r_b + \frac{3}{4}r_b^2\Delta, \qquad B = \frac{r_b(r_b+\Delta)}{2}, \quad (6)$$

$$C = \frac{r_b^2}{4}\left[1 + \left(1 + \frac{r_b\Delta}{2}\right)^{-2}\right], \qquad \alpha = \frac{r_b + \Delta}{2}. \quad (7)$$

The source term $\lambda(\xi, r_b) = -\int_0^{r_b}\rho_B(\xi, r')r'dr'$ describes the influence of driving and witness bunches, and Δ is the typical width of the electron sheath. In Refs. [15,16], a more general form of these coefficients with a function $\beta(r_b)$ is used that depends on the specific shape of the electron sheath on the boundary [18,19]. In this Letter, we use a sufficiently good approximation $\beta(r_b) = 2\Delta/r_b$.

In Figs. 2(a) and 2(b), the comparison between 3D particle-in-cell (PIC) simulations for an electron-bunch-driven bubble and the predictions of Lu's model for different values of Δ are shown (see Supplemental Material [26] for the details on PIC simulations). Equation (5) for the boundary of the bubble was solved numerically from the center position (the size and the center of the bubble are taken from simulation data) using the Runge-Kutta method of order 5(4) [27]. If Δ is chosen well ($\Delta = 0.5$ provides the best fit in this case), these equations can describe the bubble fairly accurately. However, the value of Δ cannot be found from theoretical considerations and has to be fit to better match numerical simulations. And even in the best case, a disagreement between the model and the simulations at the very back of the bubble remains. The electric field there can be more accurately described by multisheath models [22], but they increase the complexity of equations and introduce more parameters into the theory.

Equation (5) can also be simplified in the ultrarelativistic limit corresponding to $\Delta \ll r_b$ and $r_b\Delta \gg 1$ (see Ref. [16] for details). These conditions automatically mean that the bubble itself must be large, $r_b \gg 1$. In this case,

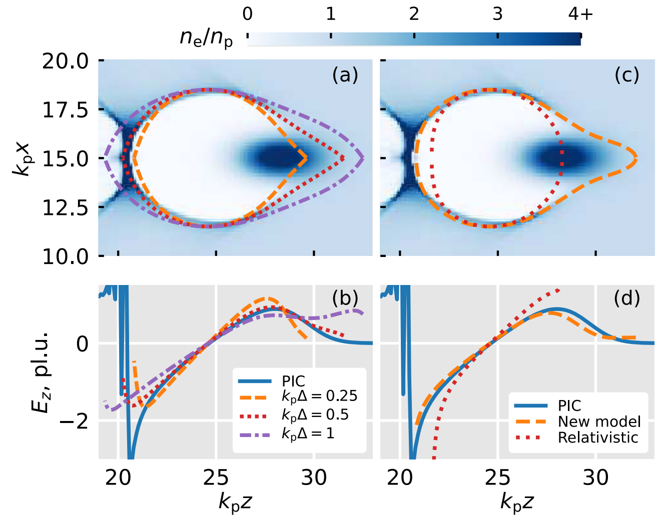

FIG. 2. The electron density distribution (a),(c) and the longitudinal electric field E_z (b),(d) in a bubble excited by an electron driver. On (a),(b), solutions for different values of Δ are calculated according to Eq. (5) with coefficients, Eqs. (6) and (7), from the previous model by Lu *et al.* On (c),(d), the dashed lines show the solution according to the new proposed model, Eq. (13), and the dotted lines show the predictions of the previous model in the ultrarelativistic limit, Eq. (8). The driver is propagating to the right and has a Gaussian shape with $k_p\sigma_r = 1$, $k_p\sigma_z = 2$, and $\rho_0 = 5$.

$$A = \frac{r_b^3}{4}, \qquad B = \frac{r_b^2}{2}, \qquad C = \frac{r_b^2}{4}, \qquad \alpha = \frac{r_b}{2}, \quad (8)$$

and the equation no longer depends on the arbitrary parameter Δ. However, due to the conditions of applicability, this simplified equation is limited to describing very large bubbles and cannot describe very small bubbles [see the dotted line in Figs. 2(c) and 2(d)].

We now use a different approach to the description of the bubble by applying the energy conservation law given by Eq. (4). To do so, we need to quantify the quasienergy densities $\tilde{W}_{\mathrm{EM}}$ and $\tilde{W}_e$. A strongly nonlinear wakefield (a bubble) is characterized by the eviction of almost all electrons and the formation of a cavity behind the driver (Fig. 1). So, we make the following assumptions: (i) the bubble has a boundary $r_b(\xi)$ within which there are no plasma electrons, i.e., $\tilde{W}_e = 0$ when $r < r_b(\xi)$, and (ii) the electron sheath on the boundary of the bubble is infinitely thin and there are no fields and no plasma motion outside the bubble for $r > r_b$, so $\tilde{W} = 0$ there. The total quasienergy in the slice $\Psi = \Psi_{\mathrm{EM}} + \Psi_e$ has contributions from the EM field and from the electrons in the sheath.

We begin with the EM field contribution. The wakefield potential satisfies the equation $\Delta_\perp\psi = j_{z,e} - \rho_e - 1$. For the infinitely thin electron sheath, no electromagnetic fields remain outside the bubble, and thus the continuity of the wakefield potential at the boundary leads to $\psi(\xi, r_b) = 0$. Inside the bubble ($r < r_b$), only the ion term equal to -1 remains, so $\psi = [r_b^2(\xi) - r^2]/4$. Therefore, the quasienergy of the EM field is

$$\Psi_{\rm EM} = \pi \int_0^{r_b} (\boldsymbol{\nabla}\psi)^2 r' \, dr' = \frac{\pi r_b^4}{16}\left[1 + 2\left(\frac{dr_b}{d\xi}\right)^2\right]. \quad (9)$$

To calculate the quasienergy Ψ_e of the electrons in the electron sheath, we consider an infinitely thin model of the sheath represented by delta functions,

$$j_z = j_0(\xi) r_b \delta(r - r_b), \qquad \rho_e = \rho_0(\xi) r_b \delta(r - r_b). \quad (10)$$

We also use the fact that the motion of plasma electrons satisfies the integral $\gamma - p_z - \psi = 1$, so $\Psi_e = -2\pi \int_{r_b-0}^{r_b+0} j_z r \, dr = -2\pi j_0(\xi) r_b^2$. The values of j_0 and ρ_0 can be found from the demand that $\int_0^\infty (j_z - \rho) r' dr' = 0$ and the assumption that electrons in the sheath are moving tangentially to the border, so that $p_r/p_z = dr_b/d\xi$. In this case,

$$j_0 = -\frac{1}{4}\left(\frac{dr_b}{d\xi}\right)^2, \qquad \Psi_e = \frac{\pi r_b^2}{2}\left(\frac{dr_b}{d\xi}\right)^2. \quad (11)$$

Thus, the total quasienergy is equal to

$$\Psi = \frac{\pi r_b^2}{16}\left[r_b^2 + (2r_b^2 + 8)\left(\frac{dr_b}{d\xi}\right)^2\right]. \quad (12)$$

The longitudinal electric field exists only inside the bubble and is given by $E_z = d\psi_\xi/d\xi = (r_b/2) dr_b/d\xi$, so Eq. (4) gives an equation for the bubble identical to Eq. (5) with

$$A = \frac{r_b^3}{4} + r_b, \quad B = 1 + \frac{r_b^2}{2}, \quad C = \frac{r_b^2}{4}, \quad \alpha = \frac{r_b}{2}. \quad (13)$$

So, by applying the energy conservation law, we arrived at an equation for the boundary of the bubble. Therefore, we can conclude that this equation is a manifestation of the fundamental law of energy conservation in plasma wakefield.

If we assume that the bubble is large ($r_b \gg 1$) and, correspondingly, almost all quasienergy is stored in the electromagnetic field ($\Psi_e \ll \Psi_{\rm EM}$), then the lower-order terms in coefficients A and B can be neglected, and we arrive at the Lu's model in the ultrarelativistic limit, Eq. (8). So, for large bubbles, the previous theory and the conservation energy approach provide exactly the same result, which was already observed in Ref. [28]. However, for smaller bubbles, the models are different. In particular, the constant term equal to 1 in the B coefficient is always absent in the previous model where B is given by Eq. (6). In addition, it can also be shown that the previous model does not have an energy integral. In fact, bubble equation (5) can be reduced to Eq. (4) if and only if its coefficients satisfy the criterion $d(A\alpha)/dr_b = 2\alpha B$. It is satisfied in the ultrarelativistic limit of the previous model, but not in the general case, so the model does not correspond to any integral. This might be the reason why it becomes so complex for smaller bubbles, as it tries to match the numerical solution using an approach that is not compatible with the fundamental energy conservation law. On the contrary, the approach based on energy conservation—even for a very simple delta-layer sheath—describes small bubbles much better than the previous theory even with a good fit for Δ [see the comparison between Figs. 2(a), 2(b) and 2(c), 2(d)]. At the same time, the coefficients in the new model remain very simple and do not depend on any arbitrary parameter, which makes this model universal.

One of the main motivations of these theoretical works is predicting the wakefield properties using only the driver parameters, without requiring any parameters taken from simulations. In a previous work by Golovanov *et al.* [23], a method for calculating the excitation of the bubble by an electron driver based on Lu's model in the ultrarelativistic limit given by Eqs. (5) and (8) was proposed. This approach, which makes it possible to calculate the bubble shape starting from the driver front, does not rely on any parameters from simulations (see the dotted lines in

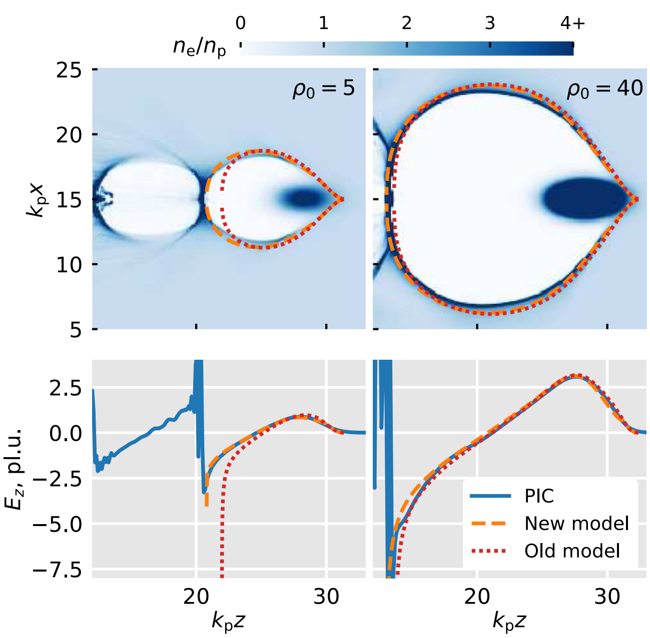

FIG. 3. Electron density distributions and the longitudinal electric fields E_z in bubbles excited by electron drivers with different peak densities ρ_0. Dashed lines correspond to the solution of Eq. (5) with coefficients, Eq. (13), from the new model [except for $r_b < 1$ where old coefficients, Eq. (8), are used instead]; dotted lines correspond to the solution with coefficients, Eq. (8), according to the approach from Ref. [23]. The drivers have a Gaussian shape with $k_p\sigma_r = 1$ and $k_p\sigma_z = 2$.

Fig. 3). However, it is based on the approximation $r_b \gg 1$ and thus provides improper results for smaller size bubbles.

The new model cannot be used for the same purpose with the method described in Ref. [23], as coefficients, Eq. (13), lead in this case to a solution $r_b = 0$, and no excitation happens. This likely owes to a nonphysical scaling of the quasienergy in the electron sheath $\Psi_e \propto r_b^2$, which completely dominates over the electromagnetic energy $\Psi_{\mathrm{EM}} \propto r_b^4$ for small values of r_b during the initial stage of excitation. In reality, this should not happen, as the sheath is not yet formed during this stage, and this scaling of Ψ_e is inadequate (for instance, in the quasilinear wake at the very front of the driver, $\Psi_e = \Psi_{\mathrm{EM}}$ instead of $\Psi_e \gg \Psi_{\mathrm{EM}}$ predicted by the model). So a proper theory describing bubble excitation should probably involve a more accurate description of the energy relations during the initial stage of excitation.

In order to self-consistently calculate the wakefield for an electron driver, we combine the approach from Ref. [23] with the new model. To do so, we calculate the solution according to Ref. [23] until the radius of the bubble reaches $r_b = r_{th} = 1$. Then we switch to the new model with coefficients, Eq. (13), assuming continuity of r_b and its derivative. Figure 3 shows the comparison of the model to numerical simulations for the electron density distributions and the longitudinal electric fields E_z for three different peak densities of the driver. More comparisons are also reported in the Supplemental Material [26] for a wider range of parameters, as well as for the case with a second (witness) bunch. The excellent agreement between the simulations and the theoretical predictions over a very wide range of parameters shows better suitability compared to the previously developed theory, while not increasing the complexity of the solved equation and not introducing additional parameters.

The new model was derived based on the energy conservation law assuming a simple delta-layer electron sheath. In principle, different shapes of the sheath can also be considered if accurate description of currents and fields outside the bubble is required. However, even the simplest shape yields exceptional similarity to PIC simulations (unlike the previous models that gave incorrect results in the limit of a delta-layer sheath). This shows the fundamental advantage of using the energy conservation approach, which gives more accurate predictions irrespective of our knowledge of the sheath properties. Thus, all future theoretical developments should take the energy conservation law into account. The new theory can also be easily generalized to transversely nonuniform plasma profiles to supersede the previous theories [20,21]. The proposed model is equally valid for the case of a laser-driven bubble in the matched regime [16] in the regions behind the driver. Using the energy conservation approach to develop a self-consistent description for a laser-driven blowout should be the next major step for the development of this theory.

The work was supported by the Ministry of Science and Higher Education of the Russian Federation (Agreement No. 075-15-2020-906, Center of Excellence “Center of Photonics”), by the Russian Foundation for Basic Research (Grant No. 20-02-00691), by The Schwartz Reisman Center for Intense Laser Physics, by Minerva, and by the Israel Science Foundation. All PIC simulations in this Letter were performed using the 3D PIC code SMILEI [29,30].

[*]Corresponding author.
anton.golovanov@weizmann.ac.il

[1] E. Esarey, C. B. Schroeder, and W. P. Leemans, Rev. Mod. Phys. **81**, 1229 (2009).

[2] I. Yu. Kostyukov and A. M. Pukhov, Phys. Usp. **58**, 81 (2015).

[3] V. Malka, J. Faure, Y. Gauduel, E. Lefebvre, A. Rousse, and K. Phuoc, Nat. Phys. **4**, 447 (2008).

[4] T. Tajima and J. M. Dawson, Phys. Rev. Lett. **43**, 267 (1979).

[5] M. J. Hogan, in *Reviews of Accelerator Science and Technology* (World Scientific, Singapore, 2017), pp. 63–83.

[6] V. Malka, S. Fritzler, E. Lefebvre, M.-M. Aléonard, F. Burgy, J.-P. Chambaret, J.-F. Chemin, K. Krushelnick, G. Malka, S. P. D. Mangles, Z. Najmudin, M. Pittman, J.-P. Rousseau, J.-N. Scheurer, B. Walton, and A. E. Dangor, Science **298**, 1596 (2002).

[7] A. Pukhov and J. Meyer-ter-Vehn, Appl. Phys. B **74**, 355 (2002).

[8] J. Faure, Y. Glinec, A. Pukhov, S. Kiselev, S. Gordienko, E. Lefebvre, J.-P. Rousseau, F. Burgy, and V. Malka, Nature (London) **431**, 541 (2004).

[9] S. P. D. Mangles, C. D. Murphy, Z. Najmudin, A. G. R. Thomas, J. L. Collier, A. E. Dangor, E. J. Divall, P. S. Foster, J. G. Gallacher, C. J. Hooker, D. A. Jaroszynski, A. J. Langley, W. B. Mori, P. A. Norreys, F. S. Tsung, R. Viskup, B. R. Walton, and K. Krushelnick, Nature (London) **431**, 535 (2004).

[10] C. G. R. Geddes, Cs. Toth, J. van Tilborg, E. Esarey, C. B. Schroeder, D. Bruhwiler, C. Nieter, J. Cary, and W. P. Leemans, Nature (London) **431**, 538 (2004).

[11] A. J. Gonsalves *et al.*, Phys. Rev. Lett. **122**, 084801 (2019).

[12] J. B. Rosenzweig, B. Breizman, T. Katsouleas, and J. J. Su, Phys. Rev. A **44**, R6189 (1991).

[13] I. Kostyukov, A. Pukhov, and S. Kiselev, Phys. Plasmas **11**, 5256 (2004).

[14] K. V. Lotov, Phys. Rev. E **69**, 046405 (2004).

[15] W. Lu, C. Huang, M. Zhou, W. B. Mori, and T. Katsouleas, Phys. Rev. Lett. **96**, 165002 (2006).

[16] W. Lu, C. Huang, M. Zhou, M. Tzoufras, F. S. Tsung, W. B. Mori, and T. Katsouleas, Phys. Plasmas **13**, 056709 (2006).

[17] M. Tzoufras, W. Lu, F. S. Tsung, C. Huang, W. B. Mori, T. Katsouleas, J. Vieira, R. A. Fonseca, and L. O. Silva, Phys. Plasmas **16**, 056705 (2009).
[18] S. A. Yi, V. Khudik, C. Siemon, and G. Shvets, Phys. Plasmas **20**, 013108 (2013).
[19] A. A. Golovanov, I. Yu. Kostyukov, A. M. Pukhov, and J. Thomas, Quantum Electron. **46**, 295 (2016).
[20] J. Thomas, I. Yu. Kostyukov, J. Pronold, A. Golovanov, and A. Pukhov, Phys. Plasmas **23**, 053108 (2016).
[21] A. A. Golovanov, I. Yu. Kostyukov, J. Thomas, and A. Pukhov, Phys. Plasmas **23**, 093114 (2016).
[22] T. N. Dalichaouch, X. L. Xu, A. Tableman, F. Li, F. S. Tsung, and W. B. Mori, Phys. Plasmas **28**, 063103 (2021).
[23] A. A. Golovanov, I. Yu. Kostyukov, L. Reichwein, J. Thomas, and A. Pukhov, Plasma Phys. Controlled Fusion **63**, 085004 (2021).
[24] B. Quesnel and P. Mora, Phys. Rev. E **58**, 3719 (1998).
[25] P. Sprangle, E. Esarey, and A. Ting, Phys. Rev. A **41**, 4463 (1990).
[26] See Supplemental Material at http://link.aps.org/supplemental/10.1103/PhysRevLett.130.105001 for details on PIC simulations and additional simulation results.
[27] J. R. Dormand and P. J. Prince, J. Comput. Appl. Math. **6**, 19 (1980).
[28] T. Wang, V. Khudik, B. Breizman, and G. Shvets, Phys. Plasmas **24**, 103117 (2017).
[29] J. Derouillat, A. Beck, F. Pérez, T. Vinci, M. Chiaramello, A. Grassi, M. Flé, G. Bouchard, I. Plotnikov, N. Aunai, J. Dargent, C. Riconda, and M. Grech, Comput. Phys. Commun. **222**, 351 (2018).
[30] SMILEI PIC code documentation, https://smileipic.github.io/Smilei/.